Progress In Electromagnetics Research C, Vol. 68, 21–30, 2016

A Novel Rectangle Tree Fractal UWB Antenna with Dual Band-Notched Characteristics

Zhangfang Hu, Yinping Hu*, Yuan Luo, and Wei Xin

Abstract—A novel rectangle tree fractal antenna (RTFA) for ultra-wideband (UWB) application with dual band notch characteristics is proposed. The radiating path is the tree fractal structure which is formed by the superposition of a number of rectangular patches, and multi-frequency resonance characteristics are obtained by only increasing the tree fractal iterations. UWB operation (3.1–10.6 GHz) is achieved by using defected ground structure (DGS) on the ground plane to improve the impedance characteristics between adjacent resonant frequencies. The dual notch bands characteristics are realized by three U-slots on the tree fractal path and effectively suppress the interferences of WiMAX and WLAN. The measurement and simulation results have an acceptable agreement, and indicate that the antenna is suitable for UWB applications.

1. INTRODUCTION

With the opening of ultra-wideband (UWB) communication system to civilian areas, UWB starts coming into people's view. The UWB system has been developed rapidly in the field of wireless communication with its advantages of high speed, high resolution, low power consumption and low interference. UWB antenna as an important component of UWB system which requires a very wide bandwidth (3.1–10.6 GHz) with good radiation characteristics and time domain characteristics has become a research hotspot. The classic UWB antennas have Vivaldi antenna [1–4] and log periodic antenna [5], etc. Vivaldi curve has a continuous gradient structure which can obtain a larger bandwidth, but it always needs a large size to achieve good performance. Literature [4] improved the design of an antipodal Vivaldi antenna which can cover a wideband from 3 GHz to 15.1 GHz, but it still has a size of $41 \times 48\,\mathrm{mm}^2$. Some special shape monopole antennas used an appropriate feeding way can also obtain a large bandwidth, such as circular monopole antennas [6, 7], hexagonal monopole antennas [8], etc. Fractal theory is a novel method for antenna design. Literature [9] summarized that fractals had highly convoluted shapes and could enhance performance when being used in antenna designs. With increasing fractal iteration there is a corresponding increase in total wire length, and a lower resonant frequency will be obtained. Lacunarity is another method to describe a fractal set. The influence of average lacunarity on antenna performance is discussed in literature [10, 11], and with increasing fractal iteration, the lacunarity and resonant frequency are gradually reduced. This analysis approach is also more practical for the non-prefractal antennas. In a word, the complexity of fractal leads to a better performance for antenna, and this complexity can be summarized as self-similarity and space filling. Lacunarity is also a characterization of space filling. The fractal antenna can obtain multiple resonant frequencies even a super-wide bandwidth because of its self-similarity. The space filling can reduce the size of the antenna [12–16], and these features are not available in other general geometries.

Received 27 July 2016, Accepted 14 September 2016, Scheduled 4 October 2016
* Corresponding author: Yinping Hu (hypcqupt@163.com).
The authors are with the College of Optoelectronic Engineering, Chongqing University of Posts and Telecommunications, Chongqing, China.

However, there are other narrowband communication systems as WiMAX (3.4–3.7 GHz) and WLAN (5.15–5.85 GHz) in the band of UWB. In order to avoid the interferences of the UWB system, an effective method is proposed to design a UWB antenna with notch characteristics. UWB antennas with notch characteristics can be achieved by a variety of ways such as using parasitic elements on the patch [17, 18] and adding quarter wavelength tuning stubs on the radiation patch or ground plane [19–23]. Cutting slot [15, 24, 25] on the patch which can change the surface current is the most common method for generating notch bands. The width of the slot is generally small, and changing the length of the slot can adjust the notch performance. The introduction of filter structures [26, 27] can also effectively suppress the interference band. The UWB antenna with multi notch bands is realized by using stepped impedance resonators [27], but the design process is more complex and with a larger size.

Fractal's self-similarity and space filling can improve performance when being used in antenna designs. Summing up the experience of UWB antenna design, it generally has a continuous gradient structure. Thus, a novel rectangle tree fractal antenna (RTFA) for UWB application is presented in this paper, and the fractal makes the antenna contain multiple resonant frequencies. The proposed RTFA covers the whole band of UWB due to the DGS ground plane which can improve the impedance characteristics between adjacent resonant frequencies. After three U-slots are cutting on the fractal patch, the dual notch band in 3.3–4.08 GHz and 5.04–6.03 GHz are realized, which can effectively restrain the interferences of the WiMAX and WLAN. The proposed antenna with a size of $30 \times 23 \times 1\,\text{mm}^3$ has good radiation characteristics, good time domain characteristics and a stable gain in the operating band.

2. DESIGN OF THE TREE FRACTAL STRUCTURE

The self-similar characteristic and complexity of fractal structure make the fractal antenna have the characteristics of multi-frequency resonance. And the bandwidth can be broadened by improving the impedance matching characteristics of adjacent resonant frequencies. The proposed rectangle tree fractal structure in this paper is formed by superposing scaled-down graphs on the two top corners of the original graph, as shown in Fig. 1. The ideal fractal structure will be formed by the infinite superposition. Fractal structure applied to the antenna design will achieve multi-frequency resonance due to those self-similar fine structures with different electric scales. The iterative process is a series of self-affine processes which can be described by an iterated function system (IFS) [12]. If (x_0, y_0) is the initial point, (x', y') is the

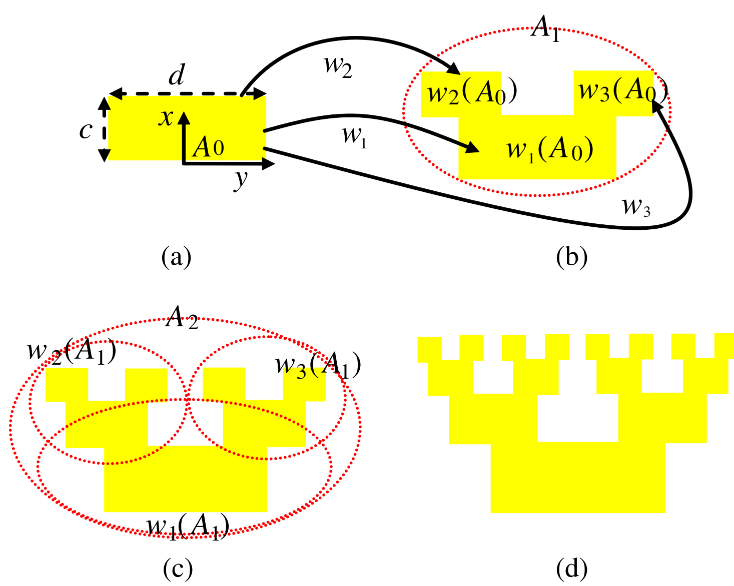

Figure 1. Iterative process of rectangle tree fractal: (a) Basic geometry. (b) First iteration. (c) Second iteration. (d) Third iteration.

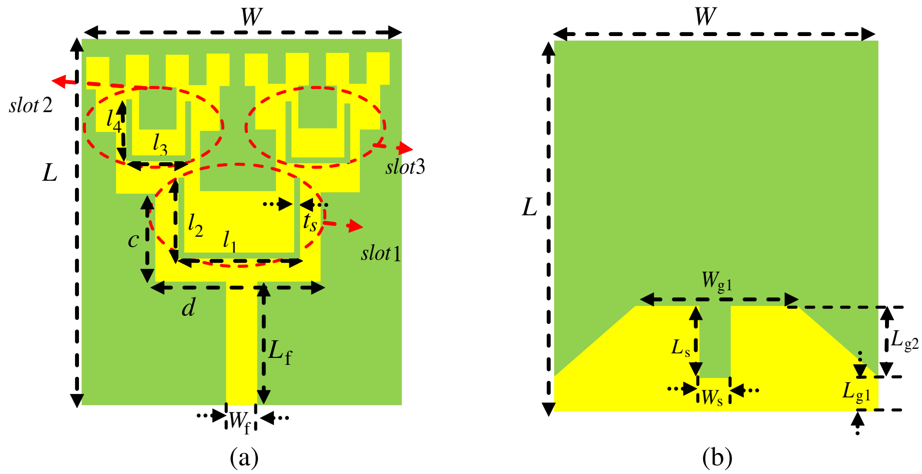

Figure 2. The structure of tree fractal antenna: (a) Top view, (b) bottom view.

point after the affine transformation, then the affine process can be expressed by the following formula

$$havew\begin{pmatrix} x' \\ y' \end{pmatrix} = \begin{pmatrix} a\cos\theta & b\sin\varphi \\ a\sin\theta & b\cos\varphi \end{pmatrix}\begin{pmatrix} x_0 \\ y_0 \end{pmatrix} + \begin{pmatrix} c \\ d \end{pmatrix} \tag{1}$$

where a and b are similarity ratios in x and y directions, respectively; θ is the rotation angle of x direction; φ is the rotation angle of y direction; c and d are the translation distances. In this paper, the iterative process of the rectangle tree-like fractal structure does not involve rotation, only the dimensional change in x direction and y direction. So, $\theta = \varphi = 0$. As shown in Fig. 1, assume that graph A_0 is a rectangular patch with a size of $d \times c$. w_1, w_2 and w_3 are self-affine transformations, which are applied to transform structure A_0, and $w_1(A_0)$, $w_2(A_0)$, $w_3(A_0)$ are obtained. Then, the tree fractal's affine process can be expressed as follows

$$w_1\begin{pmatrix} x' \\ y' \end{pmatrix} = \begin{pmatrix} 1 & 0 \\ 0 & 1 \end{pmatrix}\begin{pmatrix} x_0 \\ y_0 \end{pmatrix} + \begin{pmatrix} 0 \\ 0 \end{pmatrix} \tag{2}$$

$$w_2\begin{pmatrix} x' \\ y' \end{pmatrix} = \begin{pmatrix} a & 0 \\ 0 & b \end{pmatrix}\begin{pmatrix} x_0 \\ y_0 \end{pmatrix} + \begin{pmatrix} c \\ -d/2 \end{pmatrix} \tag{3}$$

$$w_3\begin{pmatrix} x' \\ y' \end{pmatrix} = \begin{pmatrix} a & 0 \\ 0 & b \end{pmatrix}\begin{pmatrix} x_0 \\ y_0 \end{pmatrix} + \begin{pmatrix} c \\ d/2 \end{pmatrix} \tag{4}$$

The superposition of the above will be a new geometric structure, which can be expressed as

$$W(A) = \bigcup_{i=1}^{3} w_i(A_0) \tag{5}$$

where W is the Hutchinson operator. The tree fractal will be obtained when W is repeated at the previous order graph. It can be expressed as $A_n = W(A_{n-1})$, and A_n is the n iterative fractal structure.

3. DESIGN OF TREE FRACTAL ANTENNA AND RESULT ANALYSIS

The integral structure of the RTFA for UWB operation with dual band notch characteristics is shown in Fig. 2. After simulation optimization, the specific parameters are shown in Table 1. In addition, the scaling factor $a = 0.7$, $b = 0.5$. The third order fractal structure is printed on a standard FR-4 substrate $(W \times L)$ with relative permittivity $(\varepsilon_r) = 4.4$, loss tangent $(\delta) = 0.02$ and thickness $(h) = 1$ mm. A microstrip transmission line with a strip width W_f and length L_f is used to feed the antenna. In order to improve the impedance matching characteristics in the operating band, the ground plane with a DGS structure is adopted. The DGS ground plane has two symmetrically beveling corners and a rectangular

Table 1. Design parameters of proposed tree fractal antenna (all are in mm).

W	L	W_f	L_f	c	d	t_s	l_1	l_2	l_3	l_4	L_s	W_s	L_{g1}	L_{g2}	W_{g1}
23	30	2.1	9.1	8	12	0.15	8.5	8.2	4.5	5.7	5.6	2.7	2.3	4.9	7.4

gap with a size of $L_s \times W_s$ on a rectangular ground plane. Three U-shaped slots with a width of t_s are provided on the tree fractal patch to suppress the interference due to WiMAX (3.4–3.8) and WLAN (5.15–5.85) bands.

Different iteration stages of RTFA without DGS and third iteration RTFA with DGS were simulated to analyze the influences of fractal iteration times on the performance of the antenna. Fig. 3 shows the reflection coefficients of RTFA with different iterations. The number of resonant frequencies increases, and the lowest resonant frequency decreases with an increase in the number of iterations. These will be the result of the self-similar and space-filling characteristics of tree fractal. Fig. 3 also shows the third iteration RTFA with DGS having low reflection coefficient between adjacent resonant frequencies compared to the 3 order tree fractal antenna without DGS. The bandwidth is broadened after those adjacent bands are fused together.

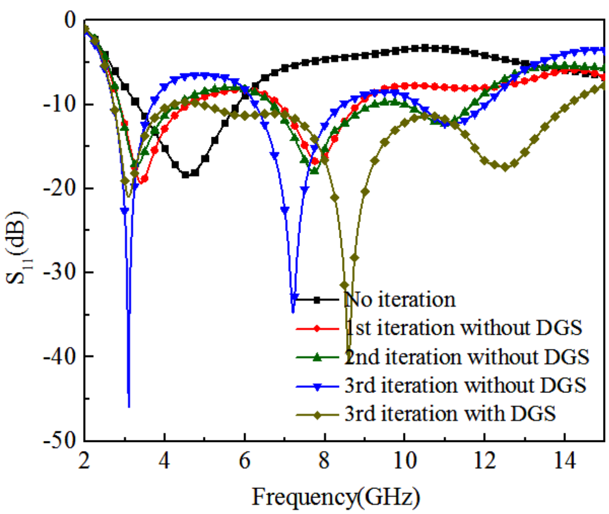

Figure 3. Reflection coefficients of the proposed antenna for different iterations.

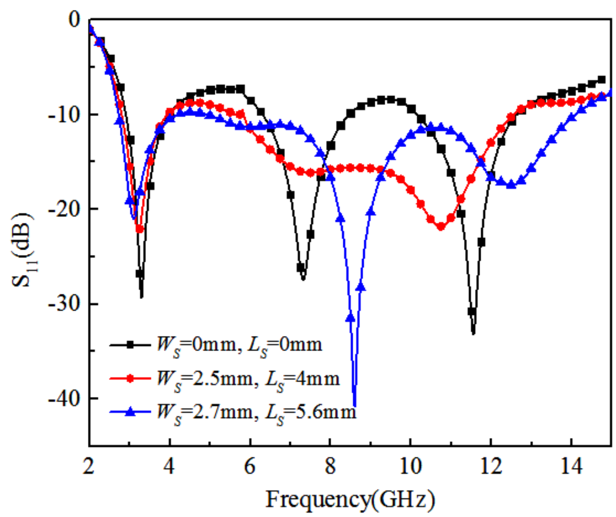

Figure 4. Reflection coefficients of the proposed antenna for different sizes of rectangular gap.

In addition, the rectangular gap in the DGS ground plane is very important to the performance of the antenna, because the capacitance introduced by the rectangular gap can offset a part of inductive capacitance of antenna and improve the impedance matching in the whole band. Fig. 4 shows the reflection coefficient for different sizes of the rectangular gap in ground plane. In this study, the sizes of the rectangular gap are divided into different groups. The values of width W_S and length L_S vary from 0 to 2.7 mm and 0 to 5.6 mm, respectively. The impedance matching of the antenna can be improved with length $L_S = 5.6$ mm and width $W_S = 2.7$ mm. From this study, we can conclude that the reflection coefficient of the operating bandwidth can be adjusted by changing the value of the rectangular gap.

The RTFA has two notch bands after three U-shaped slots are introduced. According to the principle of half-wave resonance, the slot length should be $\lambda/2$ of corresponding notch band's center frequency in the waveguide. The surface current is heavily concentrated near the slot and results in the impedance mismatch when the antenna works in the vicinity of this frequency. The relationship between the center frequency of the notch band and the length of slot is

$$f_{notch} = c/2l\sqrt{\varepsilon_{eff}} \quad (6)$$

$$\varepsilon_{eff} = (\varepsilon_r + 1)/2 \quad (7)$$

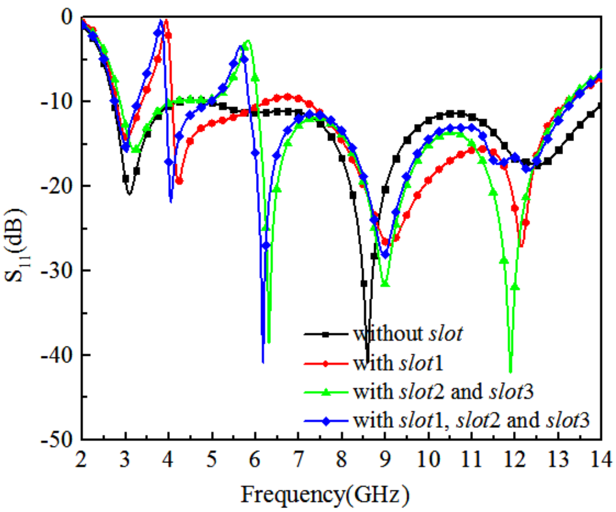

Figure 5. Reflection coefficients of the proposed antenna for different number of U-slots.

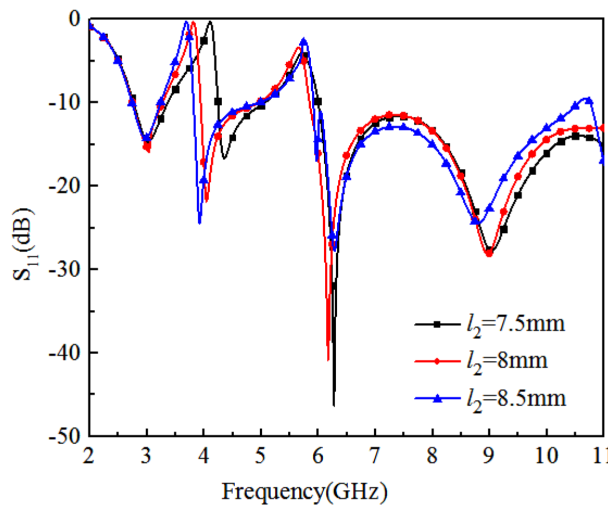

Figure 6. Reflection coefficients of the proposed antenna for different l_2.

where c is the speed of light; l is the total length of the slot; ε_{eff} and ε_r are the effective permittivity and relative permittivity. Fig. 5 shows the reflection coefficients characteristics for different numbers of U-slots. The RTFA has only a notch band near 3.5 GHz when there is only *slot*1, only a notch band near 5.5 GHz when there are only *slot*2 and *slot*3, and two notch bands near 3.5 GHz and 5.5 GHz when there are *slot*1, *slot*2 and *slot*3. Thus, it can be observed that l_{slot1} ($l_{slot1} = l_1 + 2l_2$) controls the notch near 3.5 GHz, and l_{slot2} ($l_{slot2} = l_{slot3} = l_3 + 2l_4$) controls the notch near 5.5 GHz. Fig. 6, Fig. 7 and Fig. 8 show the effect on the notch characteristics for part of the slot parameters. Fig. 6 shows the simulated reflection coefficient of the RTFA for different values of *slot*1′ length (l_2) with other parameters remaining fixed. It can be seen from Fig. 6 that l_2 has an evident effect on resonance frequency of the notch band near 3.5 GHz. It is found that the resonant frequency of the notch band near 3.5 GHz decreases with increasing values of l_2 and has no effect on the notch band near 5.5 GHz. Fig. 7 shows that the resonant frequency of the notch band near 5.5 GHz decreases with increasing values of l_4. It means that the resonant frequency of the notch band decreases with increasing size of the corresponding resonant slot. This is also consistent with formula (6). Fig. 8 shows the simulated reflection coefficient characteristics for different values of t_s. As t_s increases from 0.1 to 0.2 mm with other parameters remaining fixed, it can be observed that the notch bandwidth is increased (from the upper band edge). Hence, it can be concluded that the center frequency of the notch can be controlled by the length of slots, and the notch bandwidth can be adjusted by the width of the slots.

Figure 9 shows the fabricated RTFA for UWB operation with double notches, and the overall size of the antenna is $30 \times 23 \times 1\,\text{mm}^3$. The fabricated antenna is welded on the $50\,\Omega$ SMA connector and measured on vector network analyzer. Fig. 10 shows the measured and simulated reflection coefficients of the proposed antenna. The experimental results have some deviations compared to the simulation results due to machining error and welding error. Comparing the lower frequency edge of simulation (about 2.75 GHz) to measurement (about 2.3 GHz) shows that the lower frequency edge of the bandwidth red-shifts about 0.45 GHz in the measured results. The test shows that the operating bandwidth of the proposed RTFA covers the entire frequency band from 3.1 to 10.6 GHz, and including notch bands of 3.3–4.08 GHz and 5.04–6.03 GHz which effectively block the disturbances of the WiMAX and WLAN.

Figure 11 shows the measured and simulated radiation patterns in the E-planes (xy-plane) and H-plane (xz-plane) for 3.2 GHz, 6.5 GHz and 8.2 GHz. It can be seen that the patterns are omnidirectional at the lower-frequency band and nearly omnidirectional with back lobe at the higher-frequency band. Fig. 12 shows that the measured and simulated peak gains of the antenna are in good agreement. Measurement shows that the gain varies stably between about 2 dBi and 5.7 dBi in the operating band, and decreases sharply in two notch bands. It also confirms that the U-slots have a good blocking characteristic.

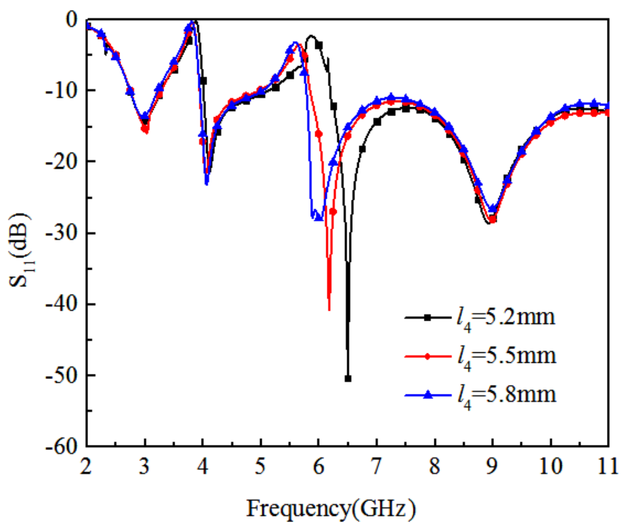

Figure 7. Reflection coefficients of the proposed antenna for different l_4.

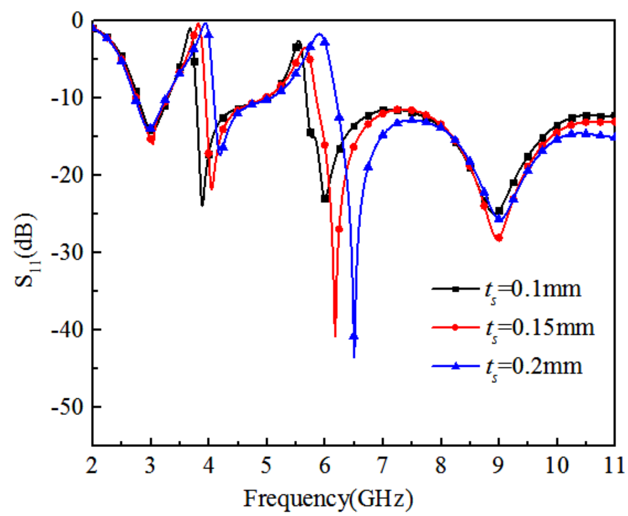

Figure 8. Reflection coefficients of the proposed antenna for different t_s.

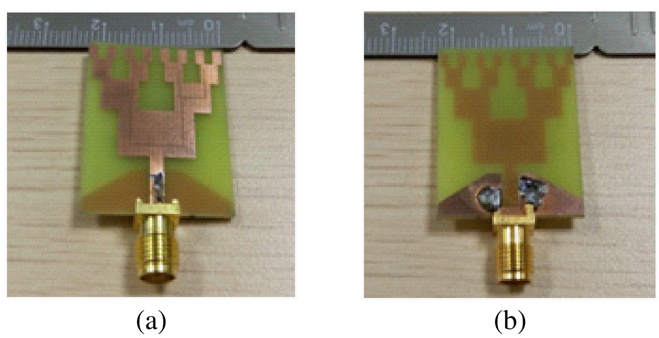

Figure 9. The fabricated tree fractal antenna: (a) top view, (b) bottom view.

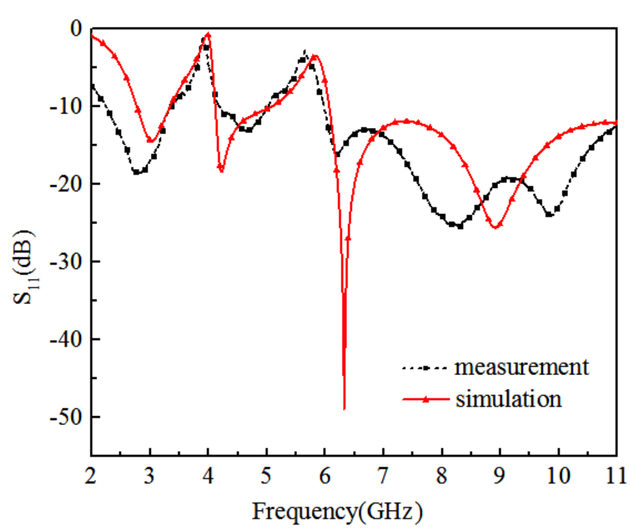

Figure 10. Simulated and measured S_{11} of the proposed tree fractal antenna.

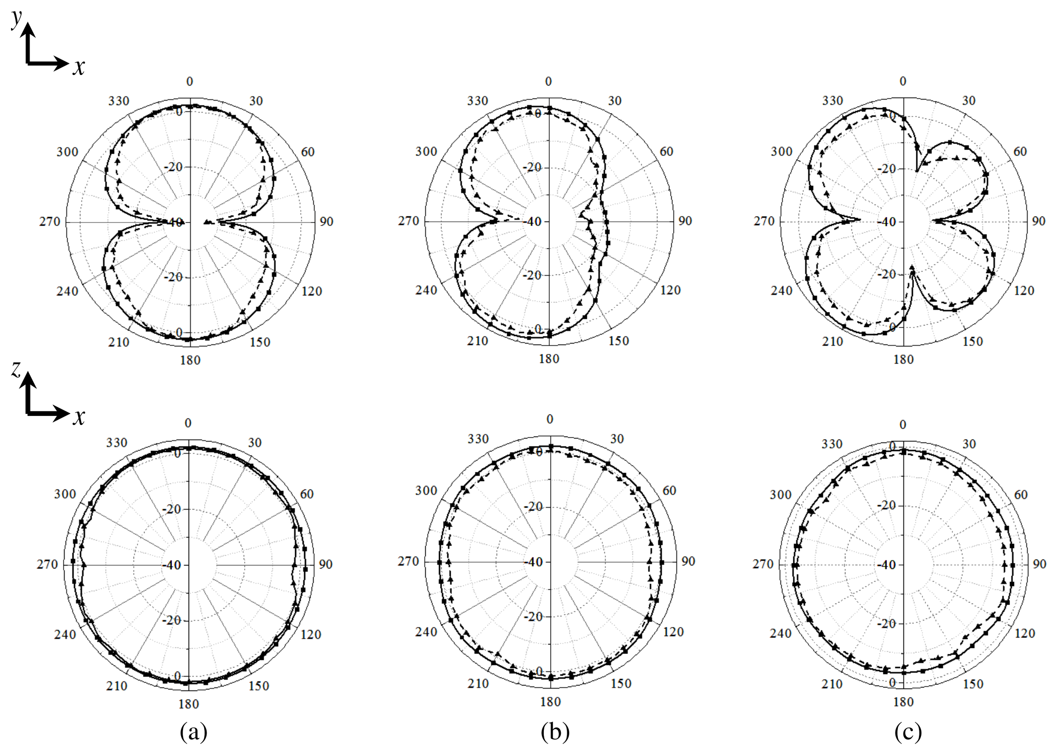

Figure 11. Measured and simulated radiation patterns for xy-plane (E-plane) and xz-plane (H-plane) for three different frequencies: (a) 3.2 GHz, (b) 6.5 GHz, (c) 8.2 GHz. (—▪— [simulation], –▲– [measurement]).

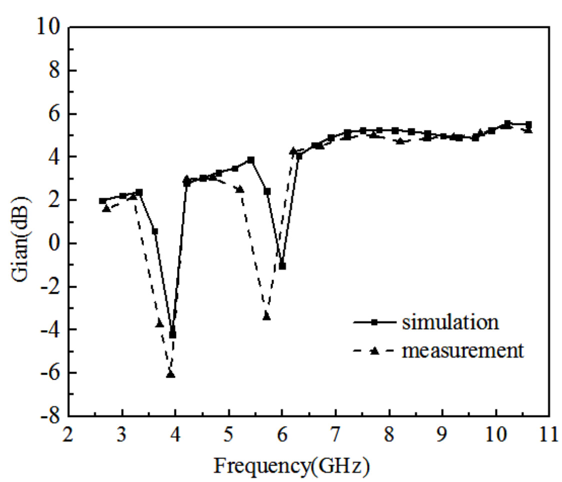

Figure 12. Measured and simulated peak gain of the antenna.

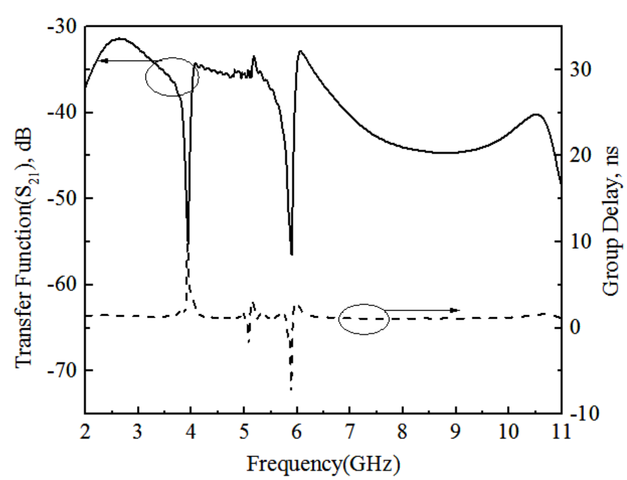

Figure 13. Group delay and transfer function of the antenna.

In order to evaluate the antenna performance in the time domain, two identical antennas are placed in the face-to-face orientation with a distance of 0.3 m (the distance should be greater than the far-field region condition) to discuss the group delay and transfer function. The transfer function is the transfer parameter S_{21} of a two-port network which should be as flat as possible in the operating band. Group delay refers to the time lag that the different frequency components reach the receiver when they transmit in the same medium. The group delay also needs to be constant over the entire band. The smaller the group delay is, the lower the signal distortion is. The formula is as follow

$$\tau = \frac{-d\varphi(\omega)}{d(\omega)} = \frac{-d\varphi(f)}{2\pi d(f)} \quad (8)$$

where $\varphi(f)$ is the frequency-dependent phase of the radiated signal. Fig. 13 displays the group delay and transfer parameter S_{21} of the antenna. It shows that group delay variation is less than 1.4 ns over the band of UWB, but it has great fluctuations in two notch bands. It also shows that the transfer parameter has a flat magnitude around −45 to −35 dB but has a sharp decrement in two notch bands. All those imply that the proposed antenna exhibits phase linearity in designed band of UWB.

Table 2. Performance summary of the other UWB antennas.

Ref	Size (mm^3)	Substrate	Operating band (GHz)	Notch Band (GHz)
3	$42 \times 36 \times 1.6$	FR4	3.7–>18	-
15	$34 \times 34 \times 1.6$	FR4	3.1–10.6	5–6
28	$50 \times 50 \times 1.575$	Taconic	2.3–>11	6.2–6.9
29	$50 \times 50 \times 1.6$	FR4	5.52–10.7	-
This work	$30 \times 23 \times 1$	FR4	2.62–>11	3.3–4.08 & 5.04–6.03

Table 2 compares the proposed antenna characteristic to some other antennas presented in [3, 15] and [28, 29]. It is clear that the proposed RTFA is smaller. Some of the other antennas are large in size, have no notch band, or cannot cover the whole band of UWB.

4. CONCLUSION

A rectangle tree fractal antenna for UWB operation is designed. Multiple resonant frequencies are obtained because of the self-similarity of tree fractal antenna. By only increasing the tree fractal iterations, new resonances are generated. UWB operation (3.1–10.6 GHz) is achieved by using DGS ground plane which can improve the impedance characteristics of antenna. The dual notch band characteristic is obtained by three U-slots on the radiation path and effectively suppressing the interferences of WiMAX and WLAN. In the notch bands, the gain decreases sharply and maintains stable in the working band. The time domain characteristics show that the proposed antenna can maintain a small distortion in the operating band. All these simulations and measurements imply that the antenna can be widely used in various UWB communication systems.

ACKNOWLEDGMENT

This work was supported in part by the Chongqing Science and Technology Commission (cstc2015jcyjB0241).

REFERENCES

1. Wu, J. N., Z. Q. Zhao, Z. Q. Nie, and Q. H. Liu "A printed UWB vivaldi antenna using stepped connection structure between slotline and tapered patches," *IEEE Antennas and Wireless Propagation Letters*, Vol. 11, 698–701, 2014.
2. Ma, K., Z. Q. Zhao, J. N. Wu, M. S. Ellis, and Z. P. Nie, "A printed vivaldi antenna with improved radiation patterns by using two pairs of eye-shaped slots for UWB applications," *Progress In Electromagnetic Research*, Vol. 148, 63–67, 2014.
3. Nassar, I. T. and T. M. Weller "A novel method for improving antipodal vivaldi antenna performance," *IEEE Transactions on Antennas and Propagation*, Vol. 63, No. 7, 3321–3324, 2015.

4. Natarajan, R., J. V. George, M. Kanagasabai, and A. K. Shrivastav, "A compact antipodal vivaldi antenna for UWB applications," *IEEE Antennas and Wireless Propagation Letters*, Vol. 14, 1557–1560, 2015.
5. Amini, A., H. Oraizi, and M. A. C. Zadeh, "Miniaturized UWB log-periodic square fractal antenna," *IEEE Antennas and Wireless Propagation Letters*, Vol. 14, 1322–1325, 2014.
6. Liang, J. X., C. C. Chiau, X. D Chen, and C. G. Parini, "Study of a printed circular disc monopole antenna for UWB systems," *IEEE Transactions on Antennas and Propagation*, Vol. 53, No. 11, 3500–3504, 2005.
7. Gong, B., J. L. Li, Q. R. Zheng, Y. Z. Yin, and X. S. Ren, "A compact inductively loaded monopole antenna for future uwb applications," *Progress In Electromagnetic Research*, Vol. 139, 265–275, 2013.
8. Dikmen, C. M., S. Cimen, and G. Cakr, "Planar octagonal-shaped UWB antenna with reduced radar cross section," *IEEE Transactions on Antennas and Propagation*, Vol. 62, No. 6, 2946–2953, Jun. 2014.
9. Steven, R. B., "A discussion on the significance of geometry in determining the resonant behavior of fractal and other non-euclidean wire antennas,"*IEEE Antennas and Propagation Magazine*, Vol. 45, No. 3, 9–28, 2003.
10. Comisso, M., "On the use of dimension and lacunarity for comparing the resonant behavior of convoluted wire antennas," *Progress In Electromagnetic Research*, Vol. 96, 361–376, 2009.
11. Sengupta, K. and K. J. Vinoy, "A new measure of lacunarity for generalized fractals and its impact in the electromagnetic behavior of Koch dipole antennas," *Fractals*, Vol. 14, No. 4, 271–282, 2006.
12. Werner, D. H. and S. Ganguly, "An overview of fractal antenna engineering research," *IEEE Antennas and Propagation Magazine*, Vol. 45, No. 1, 38–57, 2003.
13. Mahatthanajatuphat, C., P. Akkaraekthalin, S. Saleekaw, and M. Krairiksh, "A bidirectional multiband antenna with modified fractal slot fed by CPW," *Progress In Electromagnetic Research*, Vol. 95, 69–72, 2009.
14. Dhar, S., K. Patra, R. Ghatak, B. Gupta, and D. R. Poddar, "A dielectric resonator-loaded minkowski fractal-shaped slot loop heptaband antenna," *IEEE Transactions on Antennas and Propagation*, Vol. 63, No. 4, 1521–1529, Apr. 2015.
15. Choukiker, Y. K. and S. K. Behera, "Modified Sierpinski square fractal antenna covering ultra-wide band application with band notch characteristics," *IET Microwaves, Antennas* & *Propagation*, Vol. 8, No. 7, 506–512, 2014.
16. Zhao, X. Y., H. G. Zang, and G. L. Zhang, "A novel ultra-wideband fractal tree-shape antenna," *Journal of Electronic* & *Information Technology*, Vol. 37, No. 4, 1008–1012, 2015.
17. Li, T., H. Q. Zhai, and G. H. Li, "Compact UWB band-notched antenna design using interdigital capacitance loading loop resonator," *IEEE Antennas and Wireless Propagation Letters*, Vol. 11, 724–727, 2012.
18. Ojaroudi, N. and M. Ojaroudi, "Novel design of dual band-notched monopole antenna with bandwidth enhancement for UWB applications," *IEEE Antennas and Wireless Propagation Letters*, Vol. 12, 698–701, 2013.
19. Li, Y. S., W. X. Li, and Q. B Ye, "A CPW-fed circular wide-slot UWB antenna with dual-notch bands by combining slot and parasitic element techniques," *Microwave and Optical Technology Letters*, Vol. 56, No. 5, 1240–1244, 2014.
20. Weng, Y. F., S. W. Cheung, and T. I. Yuk, "Design of multiple band-notch using meander lines for compact ultra-wide band antennas," *IET Microwaves, Antennas* & *Propagation* Vol. 6, No. 8, 908–914, 2012.
21. Liu, X. l., Y. Z. Yin, P. G. Liu, J. H. Wang, and B. Xu, "A CPW-fed dual band-notched UWB antenna with a pair of bended dual-L-shape parasitic branches," *Progress In Electromagnetic Research*, Vol. 136, 623–634, 2013.
22. Gheethan, A. A. and D. E. Anagnostou, "Dual band-reject UWB antenna with sharp rejection of narrow and closely-spaced bands," *IEEE Transactions on Antennas and Propagation*, Vol. 60,

No. 4, 2071–2076, Apr. 2015.

23. Wu, Z. H., F. Wei, X. W. Shi, and W. T. Li, "A compact quad band-notched UWB monopole antenna loaded one lateral l-shaped slot," *Progress In Electromagnetic Research*, Vol. 139, 303–315, 2013.
24. Gao, P., L. Xiong, J. B. Dai, S. He, and Y. Zheng, "Compact printed wide-slot UWB antenna with 3.5/5.5-GHz dual band-notched characteristics," *IEEE Antennas and Wireless Propagation Letters*, Vol. 12, 983–986, 2013.
25. Ma, T. G. and J. W. Tsai, "Band-rejected ultra wideband planar monopole antenna with high frequency selectivity and controllable bandwidth using inductively coupled resonator pairs," *IEEE Transactions on Antennas and Propagation*, Vol. 58, No. 8, 2747–2752, Aug. 2010.
26. Zhang, Y., W. Hong, and C. Yu, "Design and implementation of planar ultra-wideband antennas with multiple notched bands based on stepped impedance resonators," *IET Microwaves, Antennas & Propagation*, Vol. 3, No. 7, 1051–1059, 2012.
27. Dong, Y. D., W. Hong, Z. Q. Kuai, C. Yu, Y. Zhang, J. Y. Zhou, and J. X. Chen, "Development of ultrawideband antenna with multiple band-notched characteristics using half mode substrate integrated waveguide cavity technology," *IEEE Transactions on Antennas and Propagation*, Vol. 56, No. 9, 2894–2901, Sep. 2008.
28. Siddiqui, J. Y., C. Saha, and Y. M. M. Antar, "Compact dual-srr-loaded UWB monopole antenna with dual frequency and wideband notch characteristics," *IEEE Antennas and Wireless Propagation Letters*, Vol. 14, 100–103, 2015.
29. Dhar, S., R. Ghatak, B. Gupta, and D. R. Poddar, "A wideband minkowski fractal dielectric resonator antenna," *IEEE Transactions on Antennas and Propagation*, Vol. 61, No. 6, 2895–2903, Jun. 2013.